

# FATIGUE CRACK GROWTH IN ADHESIVE JOINTS

D. L. Erdman, J. M. Starbuck  
Advanced Materials Processing and Measurement Technology  
Engineering Technology Division  
Oak Ridge National Laboratory  
PO Box 2009 Oak Ridge, TN 37831-8048

## ABSTRACT

Adhesive joining is recognized as a potential enabling technology for a variety of material systems being considered in automotive structures where traditional fastening methods would be inappropriate. Well known examples include fiber reinforced composites and polymers. Additionally in certain circumstances, adhesive bonding of steel structures can provide benefits such as improved stiffness and/or reduction of stress concentrations common with welded, riveted, and bolted joints. Nevertheless, there is hesitation on the part of industry to replace traditional fasteners in primary structural applications, for the most part due to the limited understanding of joint performance over the life of a structure (i.e., overall joint toughness, creep, and fatigue). Therefore, this work focuses on the fatigue crack growth in a composite-adhesive-composite joint, which could be typically encountered in an automotive structure. Methods to experimentally measure crack growth rates and quantify the growth in a useful manner are presented. This information is valuable for predicting the durability of a structure containing adhesively bonded joints.

KEY WORDS: Adhesive Joints, Double Cantilever Beam, Fatigue Crack Growth Rate

## 1. INTRODUCTION

Fatigue crack growth rate relates crack tip velocity to applied cyclic loading. This relationship in many circumstances can be used to predict the life of a structure susceptible to crack growth under cyclic loading. Standard test methods for measuring fatigue crack growth rates are well established for homogeneous, isotropic materials such as metals and plastics (1,2). These methods take advantage of analytical fracture mechanics stress analysis solutions in front of the growing crack tip, making it possible to relate cyclic stress intensity to crack growth. One popular relationship often employed is the Paris-Law equation that expresses a linear relationship between crack growth rate and stress intensity factor on a log-log scale:

$$\frac{da}{dN} = c(\Delta K)^m \quad [1]$$

where  $a$  is the crack length,  $N$  is the number of fatigue cycles,  $\Delta K$  is the cyclic stress intensity factor for a particular specimen geometry and  $c$  and  $m$  are power-law fitting constants. One example of a stress intensity solution that is applicable for the preceding equation is given below for the compact tension specimen:

$$\Delta K = \frac{(\Delta P)f(a/w)}{B\sqrt{w}}, \quad \Delta P = P_{\max} - P_{\min} \quad [2]$$

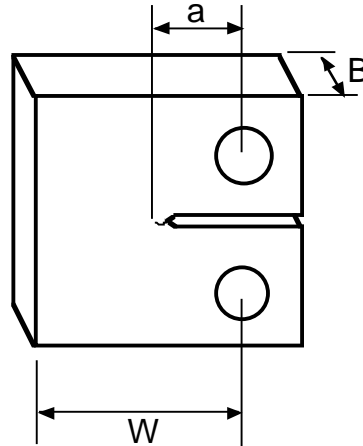


**Figure 1. Compact Tension Specimen**

The stress intensity depends on the applied dynamic load amplitude,  $\Delta P$ , specimen thickness and width,  $B$  and  $w$ , and a monotonically increasing polynomial expression,  $f(a/w)$ . It can be seen from these relationships, that as the dynamic load level increases, or the crack extends, the stress intensity increases, resulting in higher crack growth rate. Hence crack growth can be controlled through dynamic load amplitude.

In addition to the expression for  $\Delta K$ , there are well established relationships between specimen compliance (displacement-load slope) and crack lengths (compliance calibration curves). For the case of the compact specimen the relationship is given by:

$$\frac{\delta EB}{P} = CEB = F(a/w) \quad [3]$$

$$C = \frac{\delta}{P}$$

where  $\delta$  is the crack opening displacement (COD),  $C$  is the specimen compliance,  $E$  is the specimen modulus, and  $F(a/w)$  is an experimentally determined polynomial. Inversion of this relationship results in an expression for crack length,  $a$  as a function of specimen compliance. Since compliance can be determined from the load-COD slope for each cycle during a fatigue test, this provides a convenient method to monitor crack extension as an alternative to visual measurements. This capability is invaluable to automate fatigue crack growth rate tests that may run for days or weeks, and undergo millions of cycles. Although it is possible to measure fatigue crack growth rates employing visual crack growth measurements and manually adjust load levels to control crack velocity, the labor associated with the manual approach makes it very difficult if not impossible to collect the desired data throughout the entire test. Therefore, it is necessary to take advantage of the

compliance-crack length relationships to automate the testing procedure. For example, it is possible to develop testing systems with data acquisition/control software and hardware which can continuously monitor crack extension through compliance measurements, calculate stress intensity values and adjust the cyclic load levels based on these measurements to achieve the desired crack growth rate. Representative data from such a system is presented in Figure 2 below. The specimen is a 1T compact tension cast-adhesive (BFG582E), frequency =1 Hz, R=0.1.

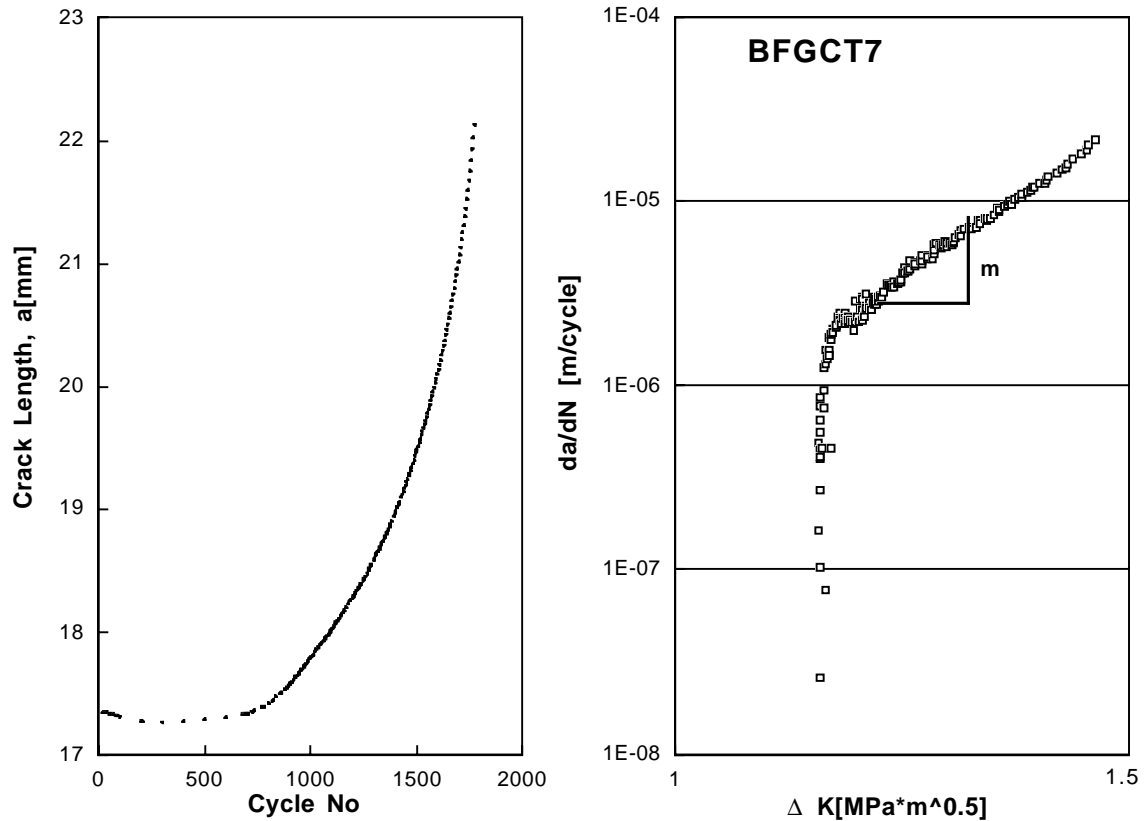
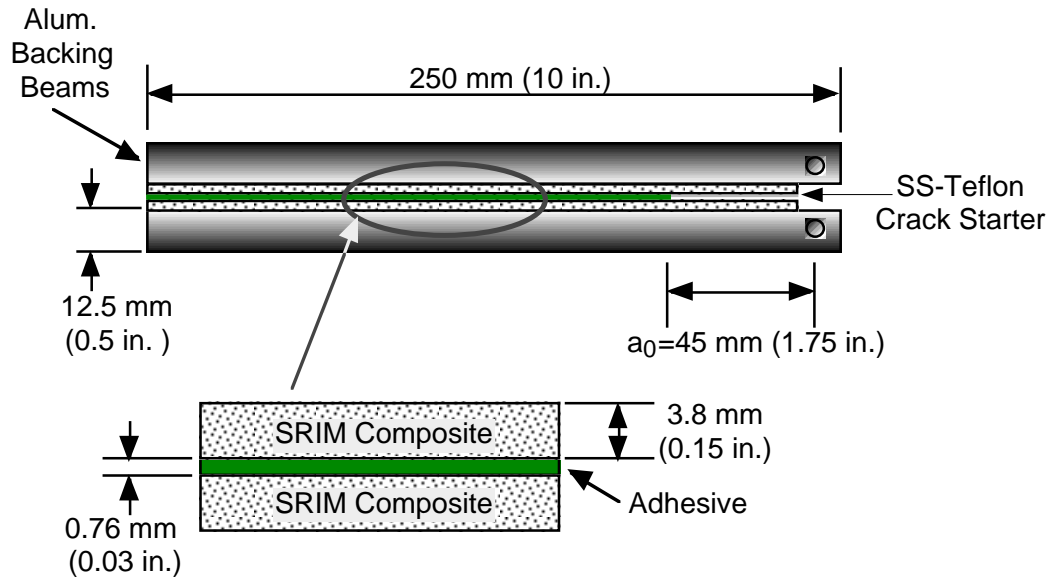


Figure 2. Fatigue Crack Growth Rate Data for a Cast Adhesive Compact Specimen

## 2. FATIGUE CRACK GROWTH RATE IN ADHESIVE JOINTS

**2.1 The Double Cantilever Beam (DCB) Adhesive Joint** For the current work, a typical adhesive joint double cantilever beam was considered as depicted in Figure 3. The specimen consists of two layers of SRIM swirled glass fiber/urethane matrix material composite bonded together with industrial adhesive (BFG582E). Aluminum backing beams were bonded to the composite to enable mode I loading through a clevis-pin arrangement, to avoid cleavage of the specimen beam arms and anti-clastic bending. A 45 mm (1.75 in.) crack starter consisting of two pieces of stainless steel shim stock separated by a Teflon strip was inserted ahead of the adhesive.

Since each beam arm consists of a combination of materials (i.e., adhesive, composite, and aluminum) a closed form stress field and associated stress intensity ahead of the crack tip is unknown. This necessitates the use of a strain energy release rate approach versus the stress intensity approach described previously.



**Figure 3. Double Cantilever Beam Adhesive Joint Specimen**

For the DCB specimen, one well known expression (3,4) for the strain energy release rate is given by:

$$G = \frac{P^2}{2b} \frac{dC}{da} \quad [4]$$

where  $P$  is the applied load,  $C$ , is the measured specimen compliance,  $a$  is the crack length measured from the load line, and  $b$  is the specimen width. It should be noted that this expression is independent of material properties and requires only specimen geometry (width) and the mechanical response of the specimen. Therefore the strain energy release rate can be calculated by using compliance measurements throughout the fatigue test. Under cyclic loading,  $G$  fluctuates with applied load:

$$\Delta G = \frac{(\Delta P)^2}{2b} \frac{dC}{da} \quad [5]$$

which is analogous to the  $\Delta K$  expressions associated with stress intensity approaches.

**2.2 Compliance Calibration for the DCB** Since the goal of this work is to study fatigue crack growth rate characteristics in the DCB, it is necessary to relate crack growth rate with cyclic load history. As with the traditional fracture specimens, developing a relationship between specimen compliance and crack length is the key to automation. For the DCB specimen, compliance is simply the ratio between the load to load-line displacement of both beam arms. Rather than relying on a purely empirical compliance calibration, a mechanics based model for the DCB was developed that considers both traditional beam bending, along with an elastic foundation solution.

Consider one half of the double cantilever beam specimen depicted in Figure 4. The model is then split in two regions, ahead of and behind the crack tip. In Region #1, an elastic foundation is employed to account for displacements and rotations that can occur due to normal and bending stresses in the compliant composite and adhesive. In Region

#2, since the two halves of the specimen are separated by the crack, the contribution to load-line displacement can be calculated from beam bending. It should be noted that this approach differs from most other approaches which consider the region behind the crack tip as a “built-in”, rigidly fixed foundation, which underestimates the load line displacement.

Within region #1, the displacement at the crack tip can be calculated by considering the resultant load and moment as shown in Figure 5:

$$\delta_1 = \frac{2\beta}{k}(1 + \beta M) = \frac{2\beta P}{k}(1 + \beta a) \quad [6a]$$

where

$$\beta = \left( \frac{k}{4EI} \right)^{\frac{1}{4}} \quad [6b]$$

$k$  is the foundation modulus and the flexural stiffness,  $EI$ , is the effective value for a composite beam consisting of several materials.

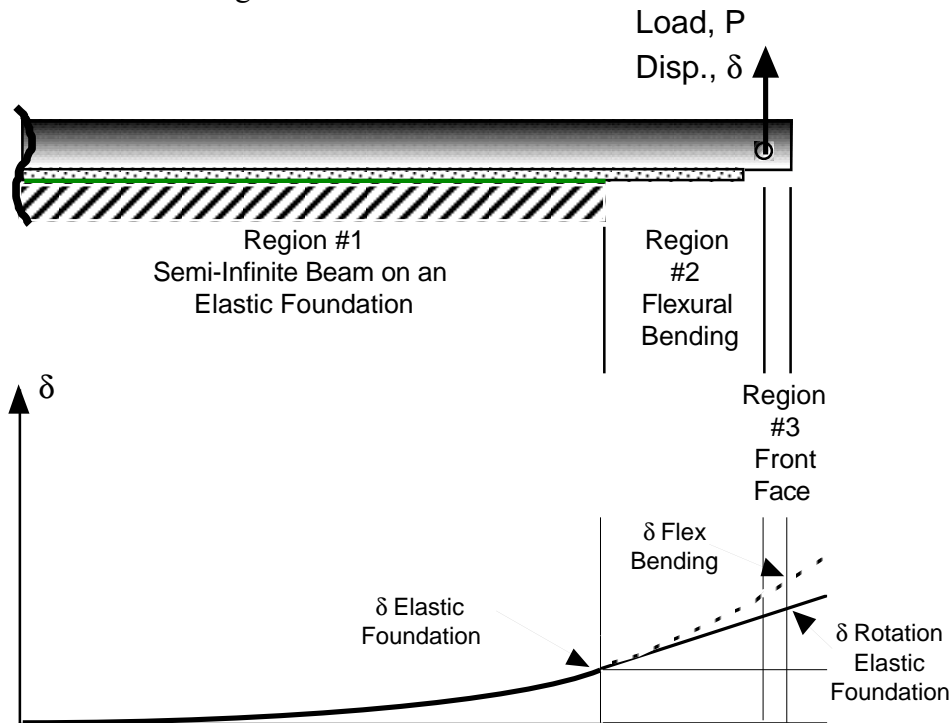


**Figure 4. Double Cantilever Beam Compliance Model and Corresponding Displacement Curves**

It should be noted that since the through thickness modulus of the composite and that of the adhesive are comparable, this portion of the analysis considers these layers “lumped” as a single layer.

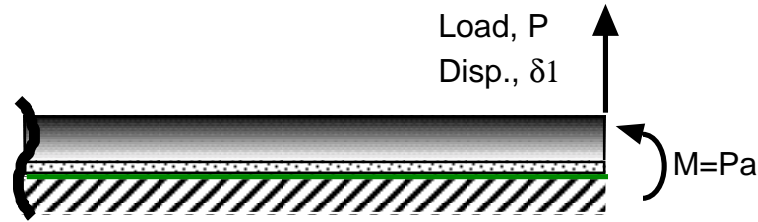


**Figure 5. Elastic Foundation Model, Region #1**

The rotation of the beam at the end of the elastic foundation (crack tip location) must also be taken into account, because it produces a rigid body rotation in Region #2 that contributes to the load-line displacement.

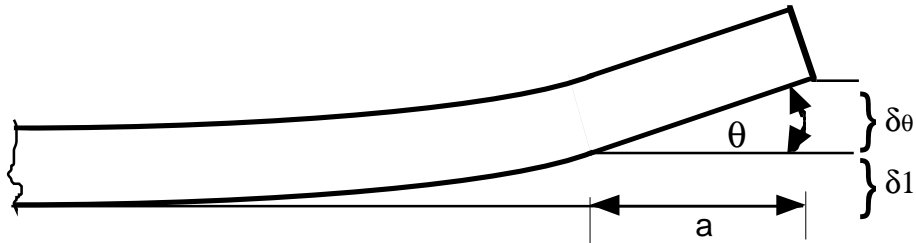


**Figure 6. Displacement at the Load-Line Due to Elastic Foundation Solution**

The rotation angle,  $\theta$  is given as:

$$\theta = \frac{2\beta^2}{k}(1+2\beta a) \quad [7]$$

and the displacement at the load line due to rotation is given as:

$$\delta_{\theta} = a \left( \tan \left\{ \frac{2\beta^2 P}{k}(1+2\beta a) \right\} \right) \quad [8]$$

It should be noted that the derivations for the results in equations 7 and 8 are covered in detail in reference (5).

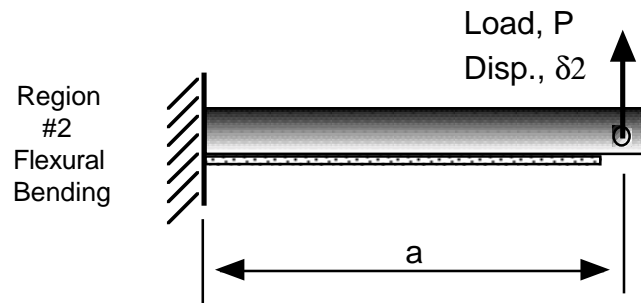


**Figure 7. Displacement Due to Bending**

In region #2, the displacement due to bending at the load-line is given as:

$$\delta_2 = \frac{Pa^3}{3EI} \quad [9]$$

Combining equations 6, 8, and 9, assuming small rotations, and writing the flexural stiffness,  $EI$  for the region ahead of and behind the crack tip in terms of  $k$ , the total specimen compliance (including both beams) is given by:

$$C = \frac{4\beta + 8\beta^2 a + 8\beta^3 a^2 + \frac{8}{3}\beta^4 a^3}{k} \quad [10]$$

The result in equation 10 provides the desired relationship to indirectly measure crack length from specimen compliance each cycle throughout a fatigue test. Inversion of this expression to solve for crack length in terms of compliance is accomplished by solving for a real, positive root of this polynomial.

**2.3 Finite Element Analysis Verification of Compliance Calibration** Finite element analyses were conducted to validate the compliance calculations based on the elastic foundation beam theory. The DCB test geometry used for the model is depicted in Figures 8 and 9.



**Figure 8. Finite Element Mesh for DCB Specimen**

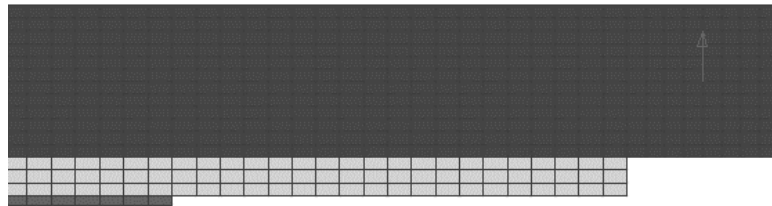


**Figure 9. Enlarged Region of Finite Element Mesh**

Symmetry considerations about the specimen mid-plane allowed modeling of a single beam arm. The mesh consisted of 4-noded (linear) quadrilateral elements, with bilinear shape functions plus incompatible shape functions (bubble functions) associated with two internal (nodeless) degrees of freedom that enable the linear element to model pure bending exactly (6). Plane stress elements were selected with a prescribed thickness equal to 12.7 mm (0.5 in.). The adhesive layer and the aluminum backing beam were modeled as isotropic materials, whereas the composite beam was modeled using orthotropic material properties. The properties values used in the EMRC NISA finite element code are provided in Table 1.

**Table I. Material Properties used in FEA**

Property	Adhesive Layer	Composite Beam	Aluminum Beam
Ex (MPa)	3172 (460 ksi)	10342 (1.5 Msi)	68950 (10 Msi)
Ey (MPa)		5171 (750 ksi)	
vxy	0.380	0.264	0.300
vxz		0.187	
vyz		0.132	
Gxy (MPa)		3613	

A unit load,  $P$ , was applied at the clevis pin hole location. The corresponding displacement at this location was used to calculate the beam compliance as a function of crack length. Crack extension was simulated by incrementally removing the displacement constraints along the mid-plane of the adhesive layer, i.e., the plane of symmetry in the finite element model. The through-thickness modulus of the composite which corresponds to the foundation modulus,  $k$  in the beam theory was set equal to 5171 MPa (750 ksi). The results from the finite element analysis are compared to the elastic foundation beam theory and experimental results from nine fatigue tests in Fig. 10. The excellent agreement between these two analyses and the experimental data indicates the elastic foundation beam theory is valid.

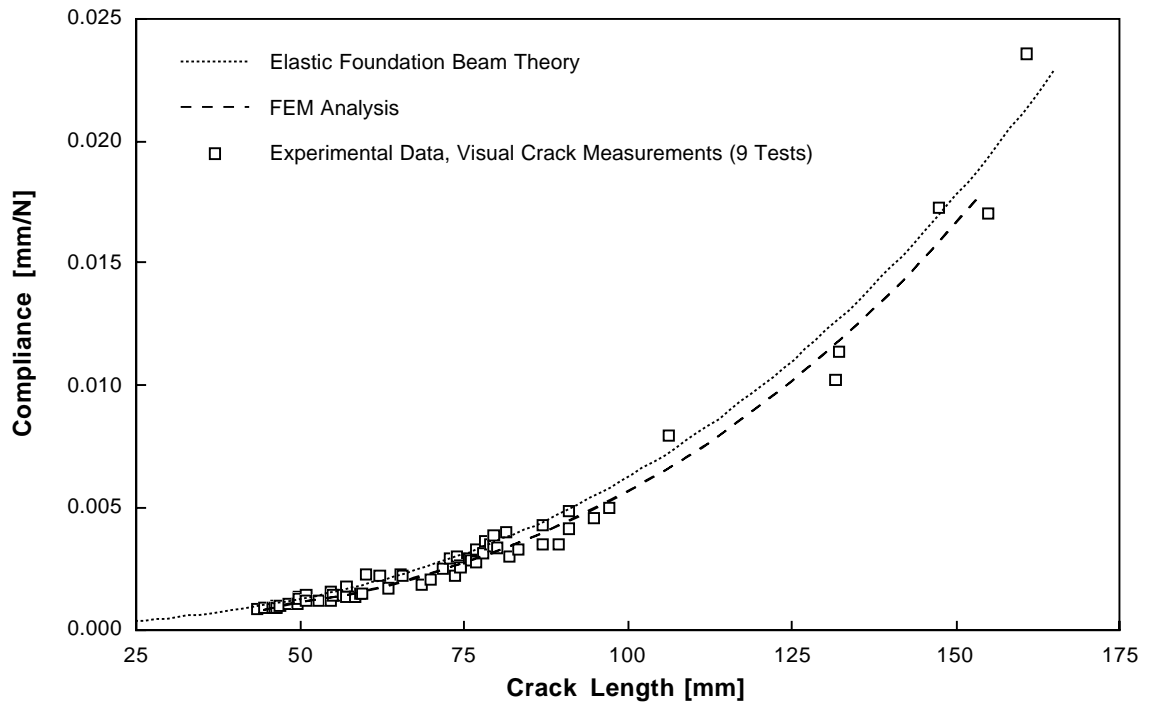


**Figure 10. Compliance vs Crack Length (Elastic Foundation Beam Theory, FEA and Experimental Data)**

**2.4 Fatigue Crack Growth Rate Expressions for the DCB Adhesive Joint** With the crack length determined from compliance measurements at each cycle, differentiation of 10 yields:

$$\frac{dC}{da} = \frac{8\beta^2 + 16\beta^3 a + 8\beta^4 a^2}{k} \quad [11]$$

which can be substituted in equation 5 along with specimen dimensions and the dynamic load level,  $\Delta P$ , to arrive at the expression for the dynamic strain energy release rate,  $\Delta G$ . To determine crack tip velocity,  $da/dN$ , a seven point incremental polynomial approach outlined in (1) was applied.

### 3. FATIGUE TESTS

Nine DCB fatigue specimens (as depicted in Figure 3) were tested to validate the compliance-crack length relationship and determine fatigue crack growth rate behavior. A summary of the specimen preparation including joint construction and backing beam attachment is described in (7).

**3.1 Test Conditions** All tests were conducted in lab-air, at room temperature in constant amplitude load control. Maximum dynamic load levels were approximately 50-60 percent of the load required to generate static crack extension in the specimen. The ratio, R of max/min sinusoidal load was 0.1.

**3.2 Test Set-Up/Apparatus** Tests were conducted on a in-house designed and fabricated servo-hydraulic test machine with a 12.7 mm (0.5 in.) stroke range, and a 1112 N (250 lb.) load range. Load line displacement was measured with a knife-edge mounted MTS clip gage having a 6.35-19.05 mm (0.25-0.75 in.) range (see Figure 11). PID control was achieved employing an MTS 407 servo-hydraulic controller. Function generation and data acquisition were accomplished by employing a National Instruments PCI-6031E 16-bit A/D-D/A board in conjunction with in-house developed LabView software. Visual crack measurements were made using magnifying lenses with halogen spot lighting.

**3.3 Test Procedure** Fatigue tests were initiated with an initial compliance check to establish a starting crack length. After crack growth initiation, visual measurements of crack length were taken periodically for comparison purposes. As the crack extended, for a number of the tests, manual load shedding in 44.5 N (10 lb.) increments were applied to determine if control of crack velocity could be achieved. After the initial stages of the test, specimen compliance was checked at least every 100 cycles and was recorded if there was a change from previous measurements of more than 1 percent. Crack lengths were allowed to extend until either the displacement range of the machine actuator or extensometer was exceeded or complete catastrophic failure of the specimen took place. During each compliance check the complete load-COD history of the cycle was recorded for post test analysis.

**3.4 Test Results** As mentioned previously, a total of nine fatigue tests were conducted. The compliance-crack length results for these tests are plotted in Figure 10. Since this testing effort was exploratory in nature, these fatigue tests were run with load shedding occurring at a different number of elapsed cycles and/or crack lengths to maximize the number of visual crack length measurements when personnel were in the laboratory. Rather than present the crack growth characteristics for each experiment, a typical fatigue crack test will be examined.



**Figure 11. DCB Fatigue Test**

Referring to Figure 12, crack growth (visual and experimentally determined from specimen compliance) is plotted as a function of elapsed cycles. As may be expected the two methods for measuring crack length are in excellent agreement throughout the test. It should be noted for this type of specimen, crack growth would be expected to occur in the adhesive layer at the mid-plane of the specimen. However, due to the relatively higher toughness of the adhesive compared to the composite material, crack growth initiates in the adhesive and proceeds to grow into the composite (approximately 1-2 mm), then continues to grow in a somewhat self-similar path parallel to the adhesive layer. For this particular test, load was shed by 10 percent, or 44 N (10 lb.) at approximately 15,000 cycles to slow the rate of crack growth. The effect of the load reduction can be observed by the corresponding change in slope of the crack extension curve, in the vicinity of the third recorded visual data point. Load was then maintained constant for the remainder of the test up to catastrophic failure. From approximately 15000-25000 cycles the crack growth has a relatively constant slope, which was found to be typical of crack growth in this composite material, in contrast to the behavior of isotropic, homogeneous, materials (Figure 2). This behavior may be attributed to the random swirled mat fiber which impedes crack growth until significant levels of damage in the composite occur ahead of the crack tip at later stages in the test.

From the plot of crack growth velocity ( $da/dN$ ) for this specimen shown in Figure 13 it can be clearly seen that crack growth velocity does not monotonically increase as might be expected under constant amplitude load conditions. Hence, there is good evidence of a complex process zone ahead of the crack tip, that most likely includes large scale yielding, fiber reinforcement and/or bridging of the crack path. Additionally, due to small-scale non-homogenous distribution of fiber in this particular composite, the crack most likely extends rapidly in the resin-rich regions of the material, and is later arrested in the regions with higher volume fractions of fiber.

This run-arrest crack behavior is exemplified in Figure 14, where, although the general trend is increasing crack growth rate with higher applied strain-energy release rates ( $\Delta G$  levels), there are significant fluctuations in the growth rate which implies a Paris-Law type description of this material is questionable (see Figure 2).

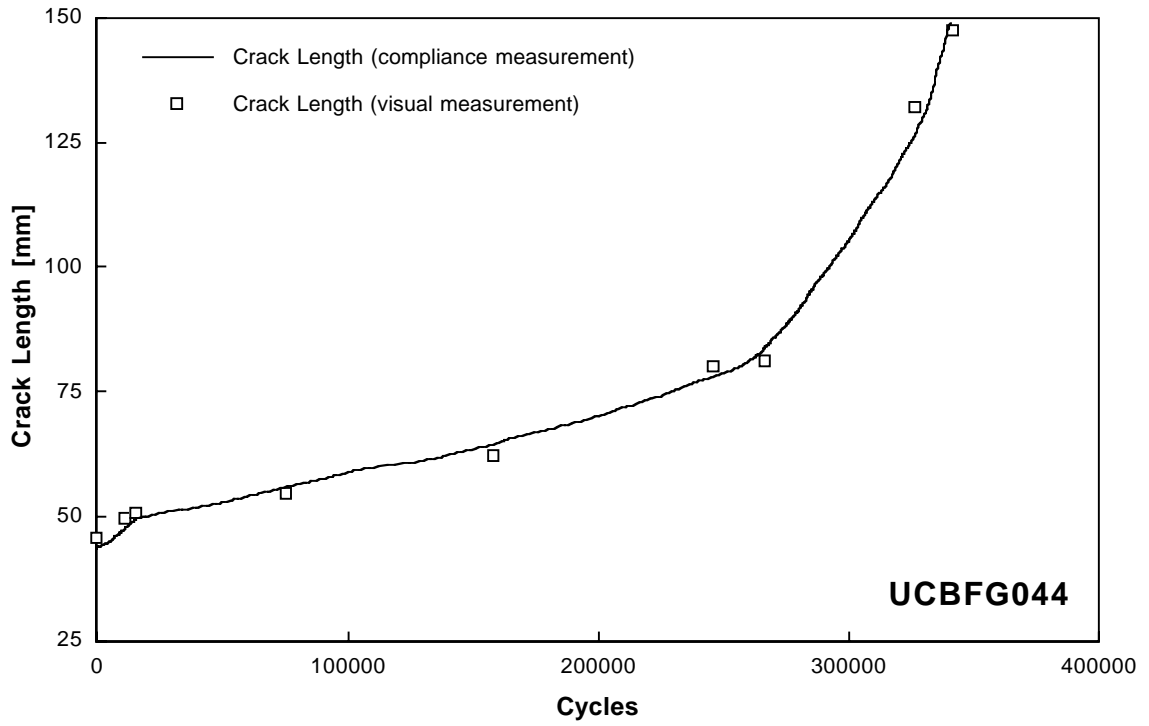


Figure 12. Crack Length vs. Number of Cycles

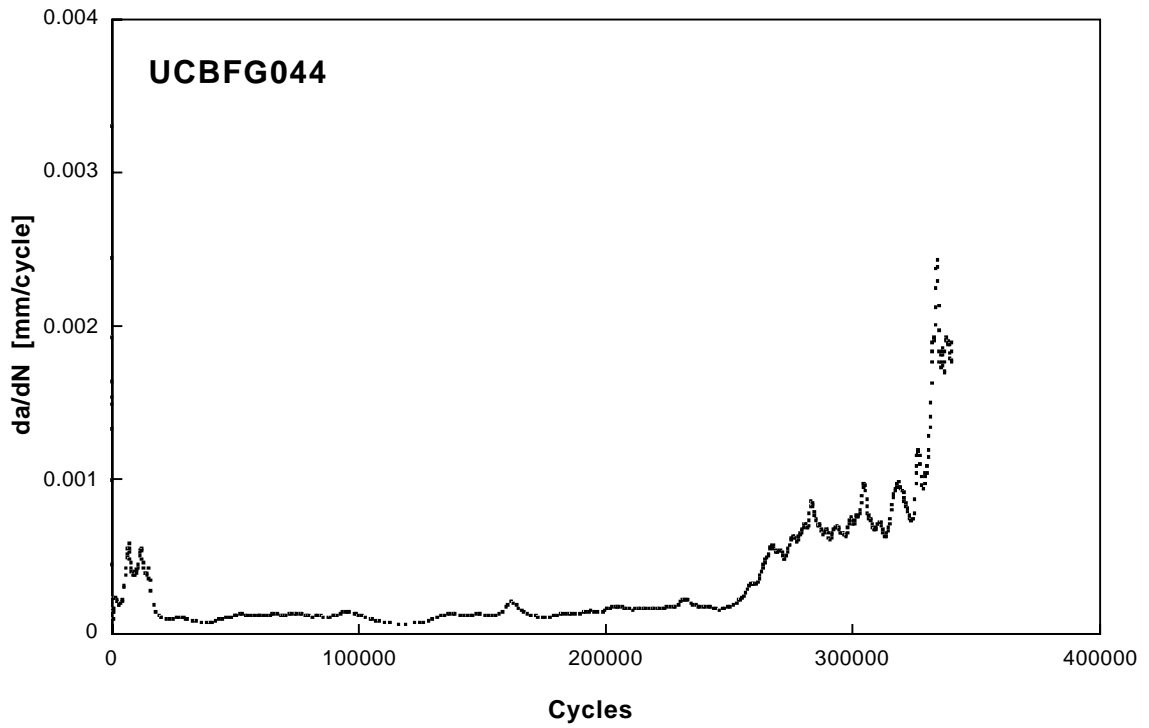
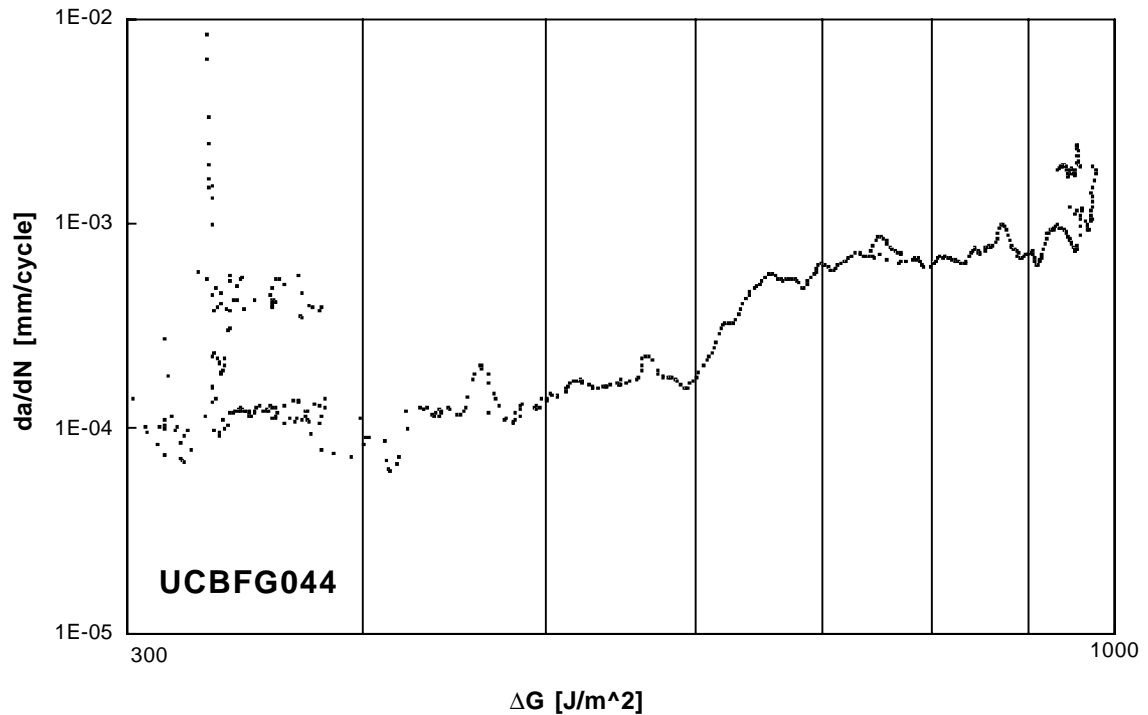


Figure 13. Crack Velocity



**Figure 14. Fatigue Crack Growth Rate**

## 4. SUMMARY

A test method for evaluating the fatigue crack growth rate behavior for adhesive joints has been presented. This method takes advantage of well established fracture mechanics practices and incorporates fundamental beam theory. A significant outcome of this work is a practical model which relates crack length with specimen compliance to automate fatigue testing and data reduction. Validity of the model is clear due to excellent correlation with experimental data and finite element results.

## 5. ACKNOWLEDGMENTS

The authors wish to thank to Ray Boeman, Ronny Lomax, Lynn Klett, and Rick Battiste of the Oak Ridge National Laboratory for assisting in the successful completion of this work. This research was sponsored by the US Department of Energy, Office of Transportation Materials, Lightweight Materials Project. Oak Ridge National Laboratory is managed by UT-Battelle for the US Department of Energy under contract DE-AC05-00OR22725.

## 6. REFERENCES

1. E647-99, Standard Test Method for Measurement of Fatigue Crack Growth Rates, Annual Book of ASTM Standards.
2. H. L. Ewalds, R. J. H. Wanhill, "Fracture Mechanics," Edward Arnold (Publishers) Ltd., 2<sup>nd</sup> Reprint, 1985.

3. J. K. Jethwa and A. J. Kinloch, "The Fatigue and Durability Behavior of Automotive Adhesives, Part 1: Fracture Mechanics Tests," *Journal of Adhesion*, 1996.
4. Leif A. Carlson and R. Byron Pipe, "Experimental Characterization of Advanced Composite Materials," Prentice-Hall Inc., 1987.
5. A. C. Ugural, and S. K Fenster, "Advanced Strength and Applied Elasticity," Elsevier, Second Edition, 1987.
6. NISA II User's Manual, Engineering Mechanics Research Corporation, Troy, Michigan.
7. Raymond G. Boeman, Donald Erdman, Lynn Klett and Ronny Lomax, "A Practical Test Method for Mode I Fracture Toughness of Adhesive Joints with Dissimilar Substrates," SAMPE-ACCE-DOE Advanced Composites Conference, Detroit, MI, September 27-28, 1999.